

# PS factor-independent and joint polarization, frequency offset and carrier phase recovery scheme for probabilistically shaped QAM

Linsheng Fan, Yanfu Yang\*, Siyu Gong, Yong Chen and Yong Yao

Department of Electronic and Information Engineering, Harbin Institute of Technology, Shenzhen, Guangdong, China

\*yangyanfu@hit.edu.cn

**Abstract:** A joint polarization, frequency offset and carrier phase recovery scheme based on frequency domain pilot is proposed for PS-QAM. Our scheme is independent of PS factor and can track polarization rotation rate up to 20Mrad/s.

## 1. Introduction

Probabilistically shaped (PS) M-quadrature amplitude modulation (MQAM) has emerged as a promising technique to deliver on better performance for coherent optical links, which allows the capacity of communication systems to approach the Shannon limit. However, the non-uniform distribution of symbols makes the DSP algorithm developed for conventional MQAM with uniform symbol probabilities perform poorly in PS-MQAM systems [1]-[3]. To take full advantage of the shaping gain brought by PS-MQAM, Zhang et al. have proposed to demultiplex the polarization of PS-MQAM in the Stokes space [4]. Yan et al. have introduced to estimate the carrier frequency offset based on radius directed-4th power algorithm [2]. Wang et al. have developed an optimized principal component-based phase estimation algorithm by mirroring and partially scaling the received constellation [5]. Nevertheless, all of the above schemes are valid for implementation with known probabilistic shaping factors (PSF). With accurate frame synchronization and decreasing of achievable information rate causing by additional overhead, data-aided DSP algorithms are also been employed in many reported PDM PS-MQAM systems [6]-[7]. However, the present algorithms for polarization demultiplexing, frequency offset and carrier phase noise recovery for PS-MQAM are handled separately in a cascaded manner. In terms of complexity and flexibility, a PSF-independent scheme with joint compensation of polarization rotation, frequency offset and carrier phase noise is preferred.

In this paper, we propose a PSF-independent scheme that can jointly compensates for polarization aliasing, frequency offset and carrier phase noise for the polarization division multiplexing (PDM) PS-MQAM system. In the proposed scheme, two frequency pilot tones (FPTs) with different frequencies are placed outside the spectrum of the modulated communication signal. The frequency offset is estimated firstly with the frequency of FPT. Then FPTs are filter out with a low pass filter (LPF) to realize the joint tracking of polarization and carrier phase. With the estimated information, the frequency offset, polarization and carrier phase noise are compensated simultaneously. To reduce the computational complexity of the DSP, the LPF is realized with a simple sliding window averaging (SWA). The performance of the proposed scheme is validated experimentally in the digital subcarrier multiplexing (DSCM) system with PS-64-QAM employing Maxwell-Boltzmann (MB) shaping. The experimental results confirmed that the PTJ scheme can tolerate ultra-fast polarization variation up to rate of 20 Mrad/s and frequency offset of  $\pm 1$  GHz without penalty of generalized mutual information (GMI).

## 2. Principle

The main idea for the proposed schemes is to insert FPTs outside the spectrum of the modulated communication signal. After propagating through the optical channel, the FPTs and signal suffer from the same impairments, including rotation of state of polarization (RSOP) caused by random birefringence, frequency offset and carrier phase noise. Consequently, Jones matrix of RSOP, frequency offset and carrier phase noise can be estimated from the FPTs. Insert a FPT in each polarization separately, the transmitted signal can be expressed as:

$$\begin{bmatrix} E_x(t) \\ E_y(t) \end{bmatrix} = \begin{bmatrix} S_x(t) + Ae^{j\omega_1 t} \\ S_y(t) + Ae^{j\omega_2 t} \end{bmatrix} \quad (1)$$

in which  $E_{x/y}(t)$ ,  $S_{x/y}(t)$  denote the transmitted and modulated signals in  $x/y$  polarization respectively.  $A$ ,  $\omega_1$  and  $\omega_2$  represent the amplitude and angle frequency of the FPTs. The power of the FPT depends on the pilot-to-signal power ratio (PSR), which is defined as  $PSR(dB) = 10\log_{10}(P_{pilot}/P_{signal})$ .  $P_{pilot}$  and  $P_{signal}$  represent the power of FPT and DSCM signal, respectively.

With negligible polarization mode dispersion and polarization dependent loss effect, the received signal can be expressed as follow:

$$\begin{bmatrix} R_x(t) \\ R_y(t) \end{bmatrix} = \mathbf{J}(t) \begin{bmatrix} E_x(t) \\ E_y(t) \end{bmatrix} e^{j(\Delta\omega t + \varphi)} + \mathbf{n}(t) = \begin{bmatrix} J_{xx}(t)(S_x(t) + Ae^{j\omega_1 t}) + J_{xy}(t)(S_y(t) + Ae^{j\omega_2 t}) \\ J_{yx}(t)(S_x(t) + Ae^{j\omega_1 t}) + J_{yy}(t)(S_y(t) + Ae^{j\omega_2 t}) \end{bmatrix} e^{j(\Delta\omega t + \varphi)} + \mathbf{n}(t) \quad (2)$$

where  $R_{x/y}(t)$ ,  $\mathbf{J}(t)$ ,  $\Delta\omega$ ,  $\varphi$ ,  $\mathbf{n}(t)$  represent the received signal in dual-polarization, the time-varying Jones matrix caused by random birefringence in fiber, the frequency offset between the signal carrier and the local oscillator, carrier phase noise and additive white Gaussian noise respectively.

The frequency offset  $\Delta\omega$  can be obtained by comparing the received FPT frequency with the transmitted one. Then, the FPTs in X and Y polarization are down-converted to the baseband respectively. A low pass filter is used to extract the FPTs for estimation of transfer matrix of RSOP and carrier phase noise. The transfer matrix  $\mathbf{W}$  can be obtained as follows:

$$\begin{bmatrix} X_{\omega_1}(t) \\ Y_{\omega_1}(t) \end{bmatrix} = \mathbf{H} \left\{ \begin{bmatrix} R_x(t) \\ R_y(t) \end{bmatrix} e^{-j(\omega_1 + \Delta\omega)t} \right\} = A \begin{bmatrix} J_{xx}(t) \\ J_{yx}(t) \end{bmatrix} e^{j\varphi} + \mathbf{H}\{\mathbf{n}(t)\} \quad (3)$$

$$\begin{bmatrix} X_{\omega_2}(t) \\ Y_{\omega_2}(t) \end{bmatrix} = \mathbf{H} \left\{ \begin{bmatrix} R_x(t) \\ R_y(t) \end{bmatrix} e^{-j(\omega_2 + \Delta\omega)t} \right\} = A \begin{bmatrix} J_{xy}(t) \\ J_{yy}(t) \end{bmatrix} e^{j\varphi} + \mathbf{H}\{\mathbf{n}(t)\} \quad (4)$$

$$\mathbf{W}(t) = \begin{bmatrix} J_{xx}(t)e^{j\varphi} & J_{xy}(t)e^{j\varphi} \\ J_{yx}(t)e^{j\varphi} & J_{yy}(t)e^{j\varphi} \end{bmatrix} \quad (5)$$

where  $\mathbf{H}\{\cdot\}$  represents the LPF operation.  $\{\cdot\}^{-1}$  represents the inverse of matrix. In Eq. (6), the constant A is removed after normalization with the total power of the FPT at the corresponding frequency ( $\sqrt{|X_{\omega_i}|^2 + |Y_{\omega_i}|^2} = A$ ). Since  $\mathbf{J}(t)$  is a unitary matrix, the matrix  $\mathbf{T}(t)$  to simultaneously recover the polarization, frequency offset and carrier phase can be expressed as  $\mathbf{T}(t) = \text{conj}\{\mathbf{W}^T\}e^{-j\Delta\omega t}$ .

Thanks to the independence between the modulated signal and the FPT, the performance of the algorithm is independent of the modulation format and PSF of the signal.

### 3. Experiment and discussions

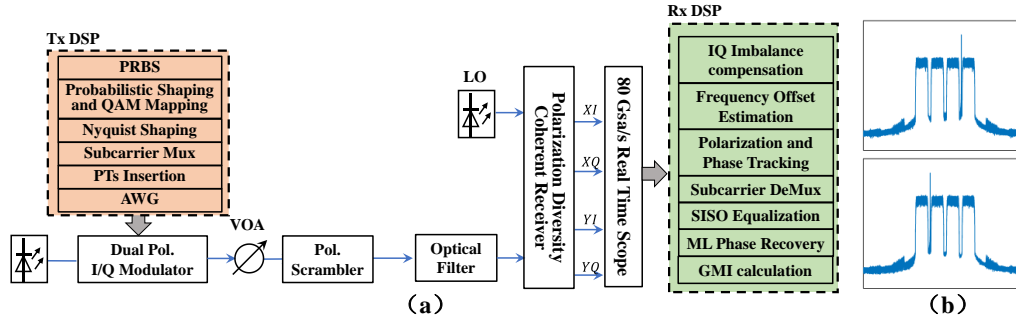


Fig. 1: (a) experimental setup and DSP flow; (b) Power spectrum of the transmitted signal

The proposed scheme is validated experimentally via PS-64-QAM employing Maxwell-Boltzmann shaping in the DSCM system. The experimental setup and DSP flow is shown in Fig. 1. In the transmitter, symbols are generated following MB-shaped 64-QAM constellations at a baud rate of 6 GBd for each subcarrier, and four subcarriers are generated with a total baud rate of 24 GBd. A root-raised-cosine (RRC) filter with a roll-off factor of 0.1 is utilized for pulse shaping. After that, subcarrier multiplexing is implemented with a guard band of 2 GHz between subcarriers. Then, two FPTs are inserted at 8.3 GHz in the X polarization and -7.6 GHz in the Y polarization, respectively. The power spectrum of the generated signals is shown in Fig. 1(b). The generated signal is converted to the analog domain via an arbitrary waveform generator (AWG: KeysightM8196A) and sent to drive the dual-polarization optical IQ modulator. A continuous-wave laser with the linewidth of 100 kHz is fed into the modulator. The modulated signals are launched into a standard single-mode fiber, and a variable optical attenuator (VOA) is used to manage the power. A polarization scrambler (EPS1000) introduces random RSOP in the fiber link. In the receiver, after coherent detection, a real-time oscilloscope (Keysight DSAZ 594A) with 80 GSA/s is used to capture the detected signals. The following DSP flow processes the captured signals. IQ skew and imbalance in the receiver side are pre-calibrated. Then, the proposed scheme is employed for joint compensation of polarization, frequency offset and carrier phase. After that, subcarrier demultiplexing is performed. An additional single input single output (SISO) based on least mean square (LMS) with nine taps and the step size of  $1e-6$  is followed to compensate for inter symbol interference (ISI) for each polarization. Then, maximum likelihood (ML) phase recovery is performed to compensate for the residual phase noise. Both the equalizer and ML phase recovery are modified to fit the PS signal. Finally, the GMI is calculated.

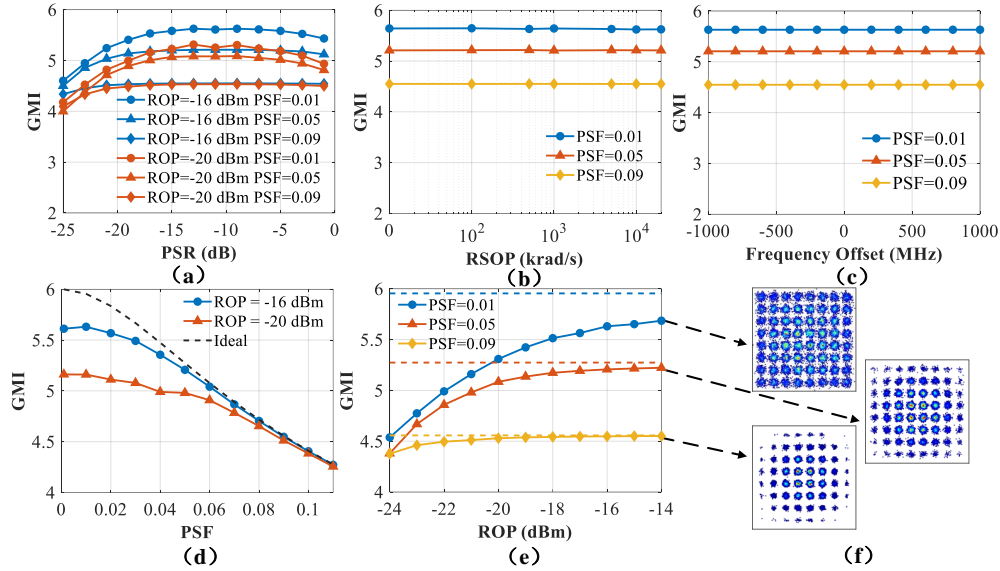


Fig.2: (a) GMI versus PSR; (b) GMI under different RSOP rate; (c) GMI under different frequency offset; (d) GMI versus PSF; (e) GMI versus ROP; (f) Constellation of different PSF at ROP = -14 dBm

Firstly, the PSR is optimized for different ROP and PSF in Figure 1. It can be seen that the GMI tends to increase and then decrease with the increasing of PSR for different received optical power (ROP) and PSF. The optimal PSR is about -13dB. The increase of PSR enhances the estimation accuracy of RSOP and phase noise, but the effective SNR will also be reduced simultaneously. The PSR is set to -13dB in the following experimental analysis.

Subsequently, the polarization tracking capability and frequency offset tolerance of the proposed scheme are discussed in Fig. 2(b) and (c), respectively. In Fig. 2(b), the ROP is set to -16 dBm and frequency offset is about 300 MHz. As can be seen, the GMI remains almost constant at different PSF as the RSOP rate increases from 0 to 20 Mrad/s. These indicate that the proposed scheme achieves ultra-fast RSOP tracking capability at different PSF. In Fig. 2(c), the ROP and RSOP rate are set to -16 dBm and 1 Mrad/s, respectively. The results show that the proposed scheme has almost no GMI penalty within  $\pm 1$  GHz frequency offset for different PSF. The above results are all achieved with the laser linewidth of 100 kHz, which indicates that the proposed scheme can jointly compensate for polarization, frequency offset and carrier phase noise.

Finally, the performance of the system is investigated at RSOP rate of 1Mrad/s and frequency offset of 300MHz for different PSF and ROP. The GMI at different PSF is shown in Figure 2(d). The gap of measured GMI at small PSF to the ideal GMI without noise mainly comes from the SNR limitation. When the PSF is greater than 0.07, the gap between the measured GMI and the ideal GMI at the ROP of -16 dBm tends to zero. Figure 2(e) shows the GMI versus ROP, the dotted line is the ideal GMI without noise for the corresponding PSF. When the PSF is greater than 0.05, the GMI at ROP = -14 dBm can approach to the ideal GMI. Figure 2(f) shows the corresponding constellation at ROP = -14 dBm. These results validate that the proposed scheme achieves joint recovery of polarization, frequency offset and carrier phase with negligible GMI reduction.

#### 4. Conclusion

In this paper, we have proposed a PSF-independent signal recovery scheme based on frequency domain pilot for PS-QAM. The scheme can achieve joint polarization, frequency offset and carrier phase recovery simultaneously. The proposed scheme is experimentally demonstrated with a 24-GBd PS-64QAM based on digital subcarrier multiplexing. The experimental results show that the GMI of the scheme at ROP = -14 dBm can approach to the ideal GMI when the PSF is greater than 0.05, which validates the effectiveness of the scheme. Meanwhile, the proposed scheme can track the polarization rotation rate up to 20 Mrad/s with negligible GMI penalty.

#### Acknowledgements

This work is supported by Shenzhen Municipal Science and Technology Innovation Council under Grants (JCYJ20190806142407195 and JCYJ20210324131408023)

#### References

- [1] S. Dris et al., Proc. OFC, Paper W1D.2, 2019.
- [2] Q. Yan et al., J. Lightw. Technol., 37(23), 5856–5866, 2019.
- [3] D. Mello et al., J. Lightw. Technol., 36(22), 5096–5105, 2018.
- [4] P. Zhang et al., J. Lightw. Technol., 39(19), 6120–6129, 2021.
- [5] X. Wang et al., J. Lightw. Technol., 38(22), 6153–6162, 2020.
- [6] D. Piloni et al., J. Lightw. Technol., 36(2), 501–509, 2018.
- [7] M. P. Yankov et al., Proc. OFC, Paper W2A.48, 2017.